

A digital filter designing tool for the Hankel and Fourier transforms in potential-, diffusive-, and wavefield modeling

Dieter Werthmüller*, Kerry Key†, and Evert C. Slob‡

ABSTRACT

The open-source code `fdesign` makes it possible to design digital linear filters for the Hankel and Fourier transforms used in potential-, diffusive-, and wavefield modeling. Digital filters can be derived for any electromagnetic method, such as methods in the diffusive limits (DC, CSEM) as well as methods using higher frequency content (GPR, acoustic and elastic wavefields). The direct matrix inversion method is used for the derivation of the filter values, and a brute-force inversion is carried out over the defined spacing and shifting values of the filter basis. Included or user-provided theoretical transform pairs are used for the inversion. Alternatively, one can provide 1D subsurface models that will be computed with a precise quadrature method using the EM modeler `empymod` to generate numerical transform pairs. The comparison of the presented 201 pt filter with previously presented filters shows that it performs better for some standard CSEM cases. The derivation of a longer 2001 pt filter for a GPR example with 250 MHz centre frequency proves that the filter method works also for wave phenomena, not only for diffusive EM fields. The presented algorithm provides a tool to create problem specific digital filters. Such purpose-built filters can be made shorter and can speed up consecutive potential-, diffusive-, and wavefield inversions.

INTRODUCTION

Deva Prasad Ghosh proposed in his Ph.D. thesis (Ghosh, 1970) a linear filter method for the Hankel transform which revolutionized the computational modeling of electromagnetic responses in the field of geophysical exploration. If you use a code that calculates electromagnetic responses in the wavenumber-frequency domain and transforms them to the space-frequency domain chances are very high that it uses the *digital linear filter* method (DLF). Ghosh (1971a) states that the idea is based on suggestions made four decades earlier by Slichter (1933) and Pekeris (1940), in that “the kernel function is dependent only on the layer parameters, and an expression relating it to the field measurements can be obtained by mathematical processes.” However, until the introduction of DLF by Ghosh these suggestions found no widespread use, probably not last because of the missing computer power to calculate the filter coefficients. He further states that credit goes to his Ph.D. supervisor Otto Koefoed (1968, 1970), who retook the task of direct interpretational methods with the introduction of raised kernel functions. DLF is, as such, an improvement of that approach, providing a faster and simpler method.

The introduction of linear filters to electromagnetic geophysics initiated a wealth of investigation, publications, and development of computer programs that extended and improved the method. A few dozen articles have been published in the 70s and 80s by Ghosh, Koefoed, Das, Anderson, and many others, the vast majority of it in the journal *Geophysical Prospecting*. Another common name of DLF is *fast Hankel transform* (FHT), popular because of the similarity of the name to the well known *fast Fourier transform* (FFT). The name was introduced, as far as we can see, by Johansen and Sørensen (1979) in their article of the same name. However, the name FHT can be misleading as it has *Hankel* in the name, but the DLF can also be applied to the Fourier transform (and other linear transforms). Publications fall broadly into one or several

*Instituto Mexicano del Petróleo, Eje Central Lázaro Cárdenas Norte 152, Col. San Bartolo Atepehuacan C.P. 07730, Ciudad de México, México, E-mail: Dieter@Werthmuller.org;

†Lamont-Doherty Earth Observatory, 305C Oceanography, 61 Route 9W, PO Box 1000, Palisades NY 10964-8000 US, E-mail: KKey@ldeo.columbia.edu; ‡TU Delft, Building 23, Stevinweg 1 / PO-box 5048, 2628 CN Delft, E-mail: E.C.Slob@tudelft.nl.

of three categories: (1) new methods (application of DLF to new measurement techniques); (2) filter improvements (new filters or providing new or improved methods for the determination of filter coefficients); and (3) computational tools. The following is a brief review of the most relevant publications regarding DLF, without claiming completeness.

(1) *New methods*

Ghosh used the method originally for the computation of type curves for Schlumberger and Wenner resistivity soundings. He published the main results of his thesis the following year in two publications: in Ghosh (1971a) he derives a resistivity model from given Schlumberger or Wenner sounding curves; and in Ghosh (1971b) he provides filters for the inverse operation, deriving resistivity sounding curves from a given resistivity model. The method was next applied to electromagnetic soundings with horizontal and perpendicular coils (Koefoed et al., 1972), to vertical coplanar coil systems (Verma and Koefoed, 1973), to dipoles and other two electrode systems (Das and Ghosh, 1974; Das et al., 1974; Das and Verma, 1980; Sørensen and Christensen, 1994), and to vertical dikes, hence vertical instead of horizontal layers (Niwas, 1975). Whilst the first filters were very specific to one type of curves and one type of transformation, various publications used the method to get one type curve from another type curve (Kumar and Das, 1977, 1978) or generalized the method to be applicable to a wider set of problems (Davis et al., 1980; Das and Verma, 1981b; Das, 1984; O'Neill and Merrick, 1984). Eventually, it passed from pure layered modeling to primary-secondary formulations in 3D problems, where DLF is used to compute the spatial Fourier-Hankel transforms in a horizontally layered background medium and to compute transient responses from frequency domain computations (Das and Verma, 1981a, 1982; Anderson, 1984; Newman et al., 1986; Kruglyakov and Bloshanskaya, 2017). Various authors delved into the theory of the method, analyzing the oscillating behaviour of the filters and trying to estimate the error of DLF (Koefoed, 1972, 1976; Johansen and Sørensen, 1979; Christensen, 1990).

(2) *Filter improvements*

Ghosh (1970) derived the filter coefficients in the spectral domain by dividing the output spectrum by the input spectrum followed by an inverse Fourier transform. Improvements to the determination of filter coefficients were provided by O'Neill (1975); Nyman and Landisman (1977); Das (1982), or specifically for the Fourier transform by Nissen and Enmark (1986). A direct integration method was used by Bichara and Lakshmanan (1976); Bernabini and Cardarelli (1978). Koefoed and Dirks (1979) proposed a Wiener-Hopf least-squares method, which was further improved by many authors (Guptasarma, 1982; Murakami and Uchida, 1982; Gupta and Singh, 1997). Kong (2007) proposed a direct matrix inversion method

to solve the convolution equation, which requires only the input and output sample values. To evaluate the filters he defines the criteria of a good filter as one that recovers small or weak diffusive EM fields. This method was also used by Key (2009, 2012). Most authors publish filters for the Hankel transform with J_0 and J_1 Bessel functions (or $J_{-1/2}$, $J_{1/2}$ if applied to the Fourier sine/cosine transform), as all higher Bessel functions can be rewritten to only use these two. Mohsen and Hashish (1994) is one of the rare cases which provides J_2 filter weights.

(3) *Codes*

The best known codes are likely the freely available ones by Anderson. Anderson (1973) extends the method to transient responses, applying DLF not only to the Hankel transform, but also to the Fourier transform. A transient signal can therefore be obtained by applying twice a digital filter to the wavenumber-frequency domain calculation. In Anderson (1975, 1979) he presents improved filters for both Fourier and Hankel transforms, introducing measures to significantly speed-up the calculation, such as the lagged convolution or using the same abscissae for J_0 and J_1 . Anderson (1982) included the 801 pt filter became sort of the industry standard, to which subsequent filters were compared. In Anderson (1989) he presents a hybrid solution, permitting to use either DLF or quadrature and as such permits to compare the two. Other examples include the codes by Johansen (1975), an interactive system for interpretation of resistivity soundings, and a tool to calculate filter coefficients by Christensen (1990). The latter is available upon request and was used, for instance, in all the open-source modeling and inversion routines of CSIRO in the Amira Project 223 (Raiche et al., 2007).

All mentioned publications have in common that they were derived for direct current methods (DC) or low frequency methods, such as time-domain shallow EM methods (TEM), or controlled-source electromagnetics (CSEM), but not for high frequency methods such as ground-penetrating radar (GPR). Generally it was even thought that the filter method works only in the diffusive limit (e.g., Hunziker et al., 2015). Also, there is no open-source filter designing tool readily available, they are available as a described method in articles or as code upon request by the author, if at all. The presented algorithm `fdesign` tries to fill this gap by providing the tools to design general or purpose-built filters using the direct matrix inversion method. After a brief overview of the methodology, the theory, and the code we show examples of its usage, presenting some new filters for both, CSEM and GPR data. The algorithm and many more examples of its usage can be found on github.com/empymod/article-fdesign. The examples can be used as templates to design new filters.

METHODOLOGY

The algorithm `fdesign` is a filter designing tool using the direct matrix inversion method as described by Kong (2007) and based on scripts by Key (2012). The tool is an add-on to the electromagnetic modeler `empymod` (Werthmüller, 2017), written in Python, and hosted on GitHub, which should foster interaction and enable anyone to toy around, improve, and extend it. It can be used to derive digital linear filters for the Hankel and the Fourier transforms for potential-, diffusive-, and wavefields (hence from DC to GPR). Theoretically, it can be used to derive linear filters for any linear transform, as long as you feed it with a theoretical, or accurately computed, transform pair of the transform. It permits to derive filters with the help of theoretical transform pairs or, alternatively, with the electromagnetic modeler `empymod`, using a quadrature method to derive accurate curves used for the inversion.

The main points of the method and some differences between it and the methods it is based upon are:

- The algorithm computes many different filters for various spacing and shift values (brute-force), with an optional minimization routine for the best outcome of the brute-force step.
- Kong (2007); Key (2012) optimize a filter for the J_0 filter, and then use the obtained shift and spacing value to calculate the J_1 values. The presented algorithm can optimize either J_0 , J_1 , or both in the optimization process. Five transform-pairs for each J_0 and J_1 , and three transform pairs for each sine and cosine of often used functions are included in the routine, but any other transform pair can be provided as input.
- More complex or more specific models can be provided instead of theoretical transform pairs by using the modeler `empymod`.
- Kong (2007) defines a *good* filter as one that recovers *weak* diffusive EM fields. In the presented algorithm you can define a relative error level which defines up to what error an obtained result is good or not. The presented algorithm can also minimize the amplitude, but it has additionally another mode, where you maximise the abscissae r of the right-hand-side of the transform pair instead of minimising the amplitude. The two modes yield the same result in the general, simple case of fast decaying transform pairs. However, if you use complex models for the design, and specifically high frequencies, then maximising r will yield much better and more consistent results.
- The algorithm allows to run under-, equal-, and over-determined systems.
- The real or the imaginary part can be used for the inversion of complex transform pairs.

The quality of a filter depends heavily on the model chosen for comparison. An obtained filter might be very good for one model, but not that good for another one, which is no different for this designing tool. There is no way to estimate the error of a result obtained with a certain filter if you apply it to any other model, unless you calculate this other model with another method for comparison. All results presented here should therefore be taken with a certain care.

Theory

Most of the articles mentioned in the review have detailed derivations of the digital filter method. In this article we focus on the algorithm, and summarize the theory only very briefly by following Key (2012). In electromagnetics we often have to evaluate integrals of the form

$$F(r) = \int_0^\infty f(l)K(lr)dl, \quad (1)$$

where l and r denote left-hand-side and right-hand-side evaluation values, and K is the kernel function. In the specific case of the Hankel transform l corresponds to wavenumber, r to offset, and K to Bessel functions; in the case of the Fourier transform l corresponds to frequency, r to time, and K to sine or cosine functions. In both cases it is an infinite integral which numerical integration is very time-consuming because of the slow decay of the kernel function and its oscillatory behaviour.

By substituting $r = e^x$ and $l = e^{-y}$ we get

$$e^x F(e^x) = \int_{-\infty}^\infty f(e^{-y})K(e^{x-y})e^{x-y}dy. \quad (2)$$

This can be re-written as a convolution integral and be approximated for an N -point filter by

$$F(r) \approx \sum_{n=1}^N \frac{f(b_n/r)h_n}{r}, \quad (3)$$

where h is the digital linear filter, and the logarithmically spaced filter abscissae is a function of the spacing Δ and the shift δ ,

$$b_n = \exp \{ \Delta(-N/2 + n) + \delta \}. \quad (4)$$

From equation 3 it can be seen that the filter method requires N evaluations at each r . To calculate for instance the frequency domain result for 100 offsets with a 201 pt filter requires 20'100 evaluations in the wavenumber domain. This is why the DLF often uses interpolation to minimise the required evaluations, either in the right-hand side (often called *lagged convolution DLF*) or in the left-hand side (*splined DLF*).

Pseudo-code

The main input variables are the filter length (N), the spacing (Δ) and shift (δ) ranges over which to loop, and

the transform pairs for the inversion (f_I) and the check of quality (f_C). If f_C is not provided, then f_I is used for both. There are additional, optional input parameters, for instance to adjust how the rhs abscissae $r = f(b, N)$ are calculated, where b is the filter base.

The basic steps are as follows:

1. Evaluate rhs of check-function f_C :
 $d_R = f_C.\text{rhs}(r)$
2. Loop over each value Δ_i, δ_j (brute force):
 - (a) Calculate filter base:
 $b_n = \exp\{\Delta_i(-N/2 + n) + \delta_j\}$
 - (b) Get required rhs (r) and lhs (l) evaluation points:
 $r = f(b, N)$
 $l = b/r$
 - (c) Invert for filter coefficients:
 $J_{ij} = \text{solve}(f_I.\text{lhs}(l), f_I.\text{rhs}(r))$
 - (d) Calculate numerically rhs of check-function f_C with current filter J_{ij} :
 $d_F = f_C.\text{lhs}(l) \cdot J_{ij} / r$
 - (e) Store minimum recovered amplitude or maximum r where relative error is less than the provided error:
 $\chi_{ij} = g[\text{argmin}(|(d_F - d_R)/d_R| > \text{error}) - 1]$,
 where g is either d_R or $1/r$.
3. Return filter coefficients which yield minimum amplitude or maximum r (a local minimization can be run to polish the brute-force result):
 return $J[\text{argmin}(\chi_{ij})]$

Minimization criteria

Figure 1 shows the differences between the different minimization approaches; in (a) for a conventional, fast decaying transform pair; and in (b) for a more complex, high frequency layered model. The circles show the minimum amplitude used in previous approaches. This criteria is not ideal, as it is subject to some random fluctuations and also depends on the choice of r . The squares show the minimum amplitude given a certain acceptable error, and the diamonds show the maximum r given a certain acceptable error (the inversion is a minimization process, it therefore minimizes $1/r$, not r). In simple cases the minimum amplitude given an acceptable error and the maximum r given an acceptable error will yield the same result. However, in complex cases the maximum r is more consistent and therefore a much better criteria.

It is important to note that independent of the inversion criteria the obtained absolute value of it is only good to compare inversion results for the same model. If you calculate filters with a different transform pair you might get very different values, but this difference says nothing about the quality of it. For instance, a certain transform pair might yield a lower minimum amplitude than

the other transform pair, but the resulting filter is worse if both filters are compared to the same transform pair. This is due to the characteristic of each transform pair.

NUMERICAL EXAMPLES

The numerical examples are focused on the Hankel transform, although `fdesign` can be used to design digital linear filters for both Hankel and Fourier transforms. As there is no difference in the procedure of the two, this should be sufficient to demonstrate the algorithm.

Design

Figure 2 shows the solution spaces of four consecutive inversion runs, where each run is a focus on a subsection of the previous run, indicated by the red square. The filter length in this case is $N = 201$, and the theoretical transform pairs are (as given, e.g., in [Anderson \(1975\)](#))

$$\int_0^\infty l \exp(-al^2) J_0(rl) dl = \frac{\exp\left(\frac{-r^2}{4a}\right)}{2a}, \quad (5)$$

$$\int_0^\infty l^2 \exp(-al^2) J_1(rl) dl = \frac{r}{4a^2} \exp\left(-\frac{r^2}{4a}\right), \quad (6)$$

where a was set to 5. In the algorithm you can provide one pair for the inversion, and a different pair to get the minimum amplitude or the maximum r . In this case the same transform pair was used for both the inversion and the check of quality. The acceptable relative error was set to 1%. The rhs evaluation parameter for the inversion was set to $r_{\text{def}} = (1, 1, 2)$, which means that an over-determined system was evaluated with $2N$ equations, where r was logarithmically spaced from $\log_{10}(1/\max(b)) - 1$ to $\log_{10}(1/\min(b)) + 1$, where b are the filter abscissae as given in equation 4.

From the low resolution overview runs (a) and (b) it looks like this is a standard, straight-forward minimization problem. However, from the more detailed results in (c) and (d) it becomes obvious that it is a minimization problem that has to be solved stochastically, as there are solutions with 2 orders of magnitude difference apparently randomly next to each other.

Figure 3 shows in (a) the filter values for J_0 and J_1 of the best 201 point filter obtained this way, and in (b) its right-hand-side solution. The black dots indicate negative values, from which it can be seen that adjacent values are often alternating between positive and negative contributions.

Designing filters is to a large extent trial and error. All input variables influence the outcome, and often you will come across a good filter by sheer luck of choosing the right starting parameters. Each of the input parameters has an effect to the outcome. It depends a lot on the transform pairs $f_{I,C}$, and functions that decay rapidly are generally better, as noted by earlier authors (e.g. [Anderson, 1975](#)). It also depends on the filter length, and obviously heavily on the spacing and shift values, as this is what we

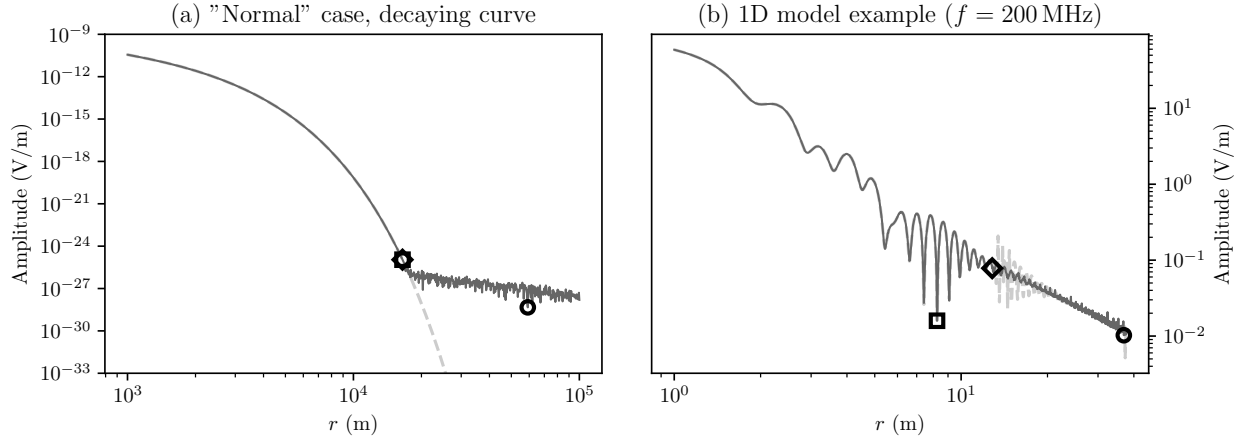


Figure 1: (a) A regular rhs curve of a transform pair with a purely decaying function. Minimum amplitude or maximum r yield the same result in this scenario. Using a relative error criteria is more stable than just the absolute minimum amplitude. (b) A 1D model for $f = 80$ MHz. Here, the maximum r provides a better criteria for the inversion.

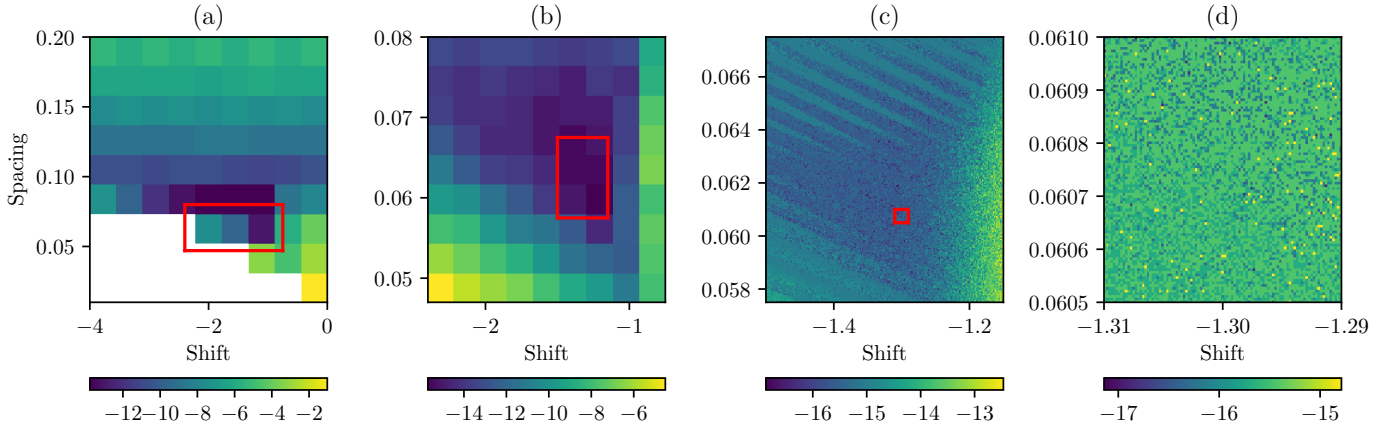


Figure 2: Solution spaces of four consecutive inversion runs for a 201 pt filter. Each consecutive run zooms into a portion of the previous solution space, indicated by the red square. The more in detail we obtain the solution space, the more random appears to be the distribution.

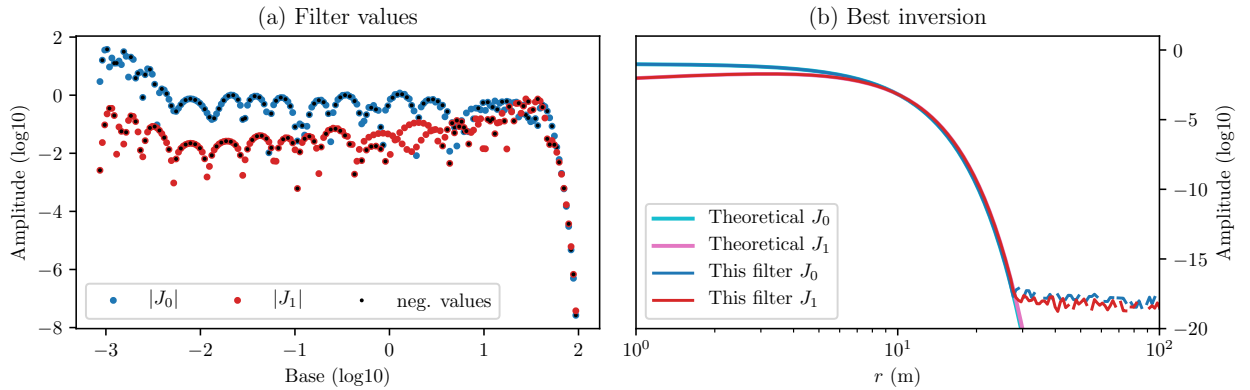


Figure 3: (a) Filter values of the best obtained 201 pt filter with the corresponding check of quality in (b). Black points indicate negative values, which shows that adjacent values have often opposite signs.

invert for. Another important point is how you define the right-hand evaluation points of the inversion (r_{def}). Evaluating corresponding transform pairs separately or jointly also leads to different filter coefficients (J_0 , J_1 , or J_0 & J_1 , or equally sine, cosine, or sine & cosine); also if the real or the imaginary part is used when complex transform pairs or `empymod` is used; and if it is inverted for the minimum amplitude or for the maximum r .

CSEM

In this section we compare the 201 pt filter derived in the previous section to CSEM models used in Kong (2007), Key (2012), and a land case.

Figure 4 compares the derived 201 pt filter with the two half-spaces case used by Kong (2007) in his figure 5. The model consists of a water layer with $\rho_w = 0.3125 \Omega \text{m}$ of infinite thickness above a subsurface half-space with $\rho = 1 \Omega \text{m}$. The signal of an x -directed electric source 50 m above the interface is measured at an x -directed electric receiver at the interface, frequency is $f = 1 \text{Hz}$. In (a) it can be seen that the new 201 pt filter is able to recover smaller amplitudes than the 241 pt filter from Kong (2007), the 201 pt filter from Key (2012), and the 801 pt filter from Anderson (1982) (Wer201, Kong241, Key201, and And801, respectively). It behaves equally well as the quadrature with extrapolation (QWE), for which we used a 51 pt quadrature with relative and absolute tolerance of $1\text{e-}12$ and $1\text{e-}30$, respectively. The relative error is shown in (b), where the QWE result was taken as *truth*. For offsets greater than roughly 15.5 km the relative error becomes meaningless, as the QWE fails itself; this part is greyed out in the figure.

Figure 5 (a) is the canonical CSEM model as used in Key (2012) in his figure 5: Water depth of 2 km with $\rho_w = 0.303 \Omega \text{m}$, a background resistivity of $\rho_b = 1 \Omega \text{m}$, in which a target is embedded of $\rho_t = 100 \Omega \text{m}$ at 1000 m below the seafloor, 100 m thick. Source depth is 1990 m, receivers are on the seafloor. Figure 5 (b) is a land case, with a background resistivity of $\rho_b = 10 \Omega \text{m}$, in which a target is embedded of $\rho_t = 500 \Omega \text{m}$ at 1000 m below the surface, 100 m thick. Source depth is 0.5 m, receiver depth is 0.8 m. In both cases the new filter *Wer201* has generally a relative error which is orders of magnitude lower than the other filters. The relative error of the real part is given in black, whereas the relative error of the imaginary part is given in grey. It is interesting to note that the real and imaginary parts have very similar errors in *Wer201*, *Key201*, and *And801*, but that the imaginary part of *Kong241* seems to behave considerably better for most part than its real counterpart. To compare the real and the imaginary parts is insofar interesting as the digital filters are purely real valued.

It is very important to note again that other scenarios might yield very different error plots. Although the new 201 pt filter proves to be very accurate for these three models, it might not be the best filter in other cases.

Ground-penetrating radar

Figure 6 shows the GPR example as calculated in Hunziker et al. (2015); Werthmüller (2017); the model parameters are given in subplot (a). The filter used for this example for the Hankel transform is a 2001 pt filter, derived with the fullspace solution with $f = 500 \text{MHz}$ for the inversion and the check of quality. Vertical source and receiver separation is 1 m, resistivity $\rho = 200 \Omega \text{m}$, $\epsilon_r = 10$, $\mu_r = 1$. For the Fourier transform a 4096 pt FFT was used with regularly spaced frequencies from 0.5 MHz to 850 MHz and then zero-padded up to 2048 MHz for both the calculation with the adaptive quadrature (QUA) and with the DLF. The frequency result is multiplied with a Ricker wavelet with a center frequency of 250 MHz, and a gain function $(1 + |t^3|, t \text{ in ns})$ is applied. The calculation with the digital filter took under 9 minutes and is therefore roughly 80 times faster than the adaptive quadrature calculation which took roughly 11 hours and 27 minutes. Calculating the same model with QWE took 7 hours and 20 minutes. However, QWE uses in roughly 1/3 of the calculation internally the adaptive quadrature in this example, see Werthmüller (2017). (Note that DLF was run in parallel using 4 threads at once, taking effectively only 2 minutes and 10 seconds to calculate. The lagged convolution version of DLF and the splined version of QWE were used in this comparison.)

Figure 7 shows in (a)-(c) the real part of the frequency domain results and in (d)-(f) the time domain results for offsets of 0.2 m, 2.0 m, and 3.0 m.

The 2001 pt filter was derived with the fullspace solution of a medium which is very similar to the layer in which source and receiver reside in our GPR example. To show that this filter can also be applied to different layer parameters we run a test where we swapped layers one and two of the model in Figure 6 (a). The resulting real and imaginary parts for the offsets 0.2 m, 2.0 m, and 3.0 m are given in Figure 8.

These examples show clearly that the filter method can indeed be applied to high frequency EM modeling and therefore wave phenomena. We are convinced that with further tests and analysis much better filters could be achieved, and various concepts could be checked. One approach is to derive a filter for each frequency band, say one for 1 MHz–10 MHz, one for 10 MHz–100 MHz, and one for 100 MHz–1 GHz. Another approach could be to derive distinct filters for J_0 and J_1 , with different spacing and shift values. The first idea would triple the calculation cost, the second idea double them; however, they both would still be very fast compared to standard quadrature methods. One could also apply the digital filter method to acoustic and elastic wavefields as well.

CONCLUSIONS

The presented, free and open-source code `fdesign` can be used to design digital linear filters for the Hankel and Fourier transforms (and more generally for any linear trans-

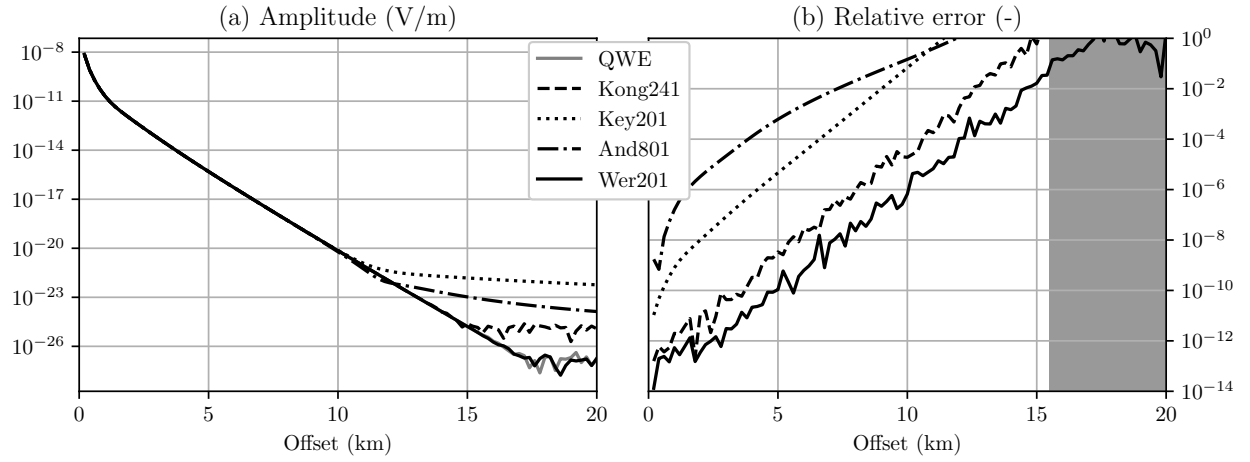


Figure 4: (a) Results of different filters and QWE for the model of figure 5 from Kong (2007) with the relative errors shown in (b), using the QWE result. The relative error is meaningless from about 15.5 km onwards, as QWE failed as well for these very low amplitudes.

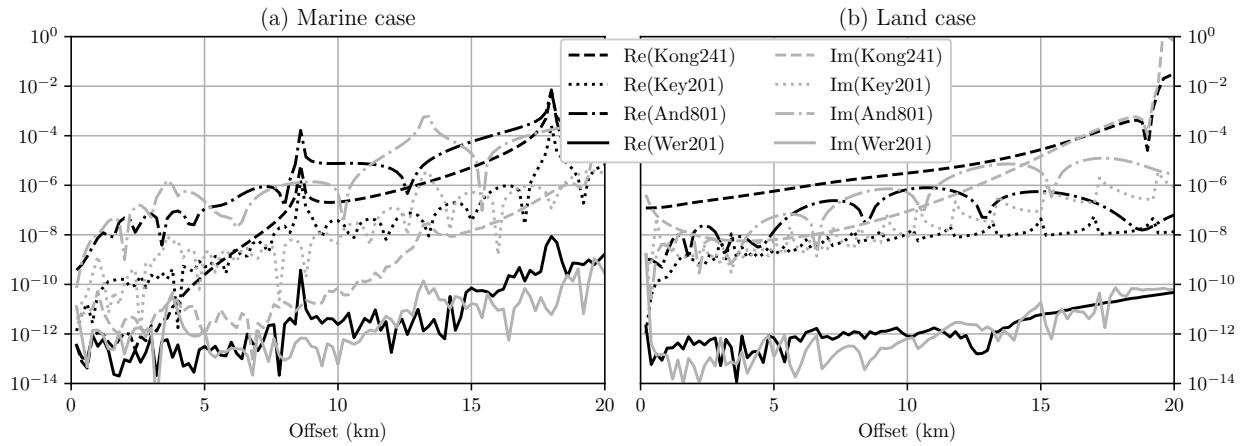


Figure 5: (a) The canonical marine CSEM model of Key (2012) and (b) a land model with source and receiver at the surface. The new filter has generally relative errors which are several orders of magnitude lower than the other filters.

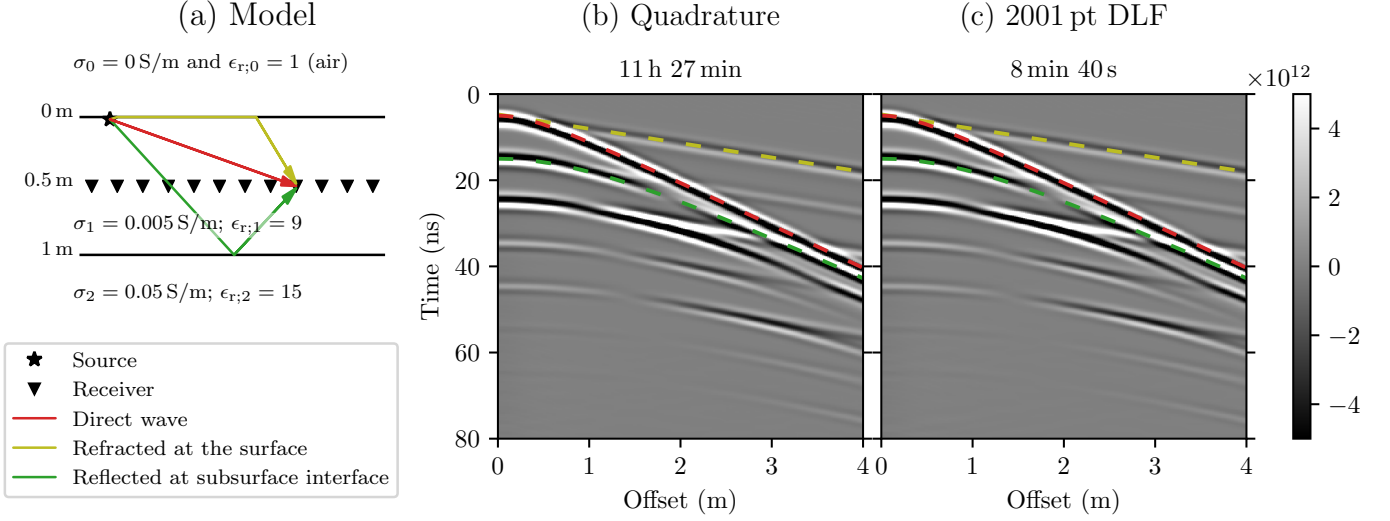


Figure 6: GPR example for the model given in (a) using `empymod` with (b) the adaptive quadrature (QAGSE from the Fortran QUADPACK library) or with (c) a 2001pt digital linear filter (b). The quadrature took about 11 h 27 min to calculate, whereas the filter took 2 min 10 s in parallel on 4 nodes, hence under 9 min in total.

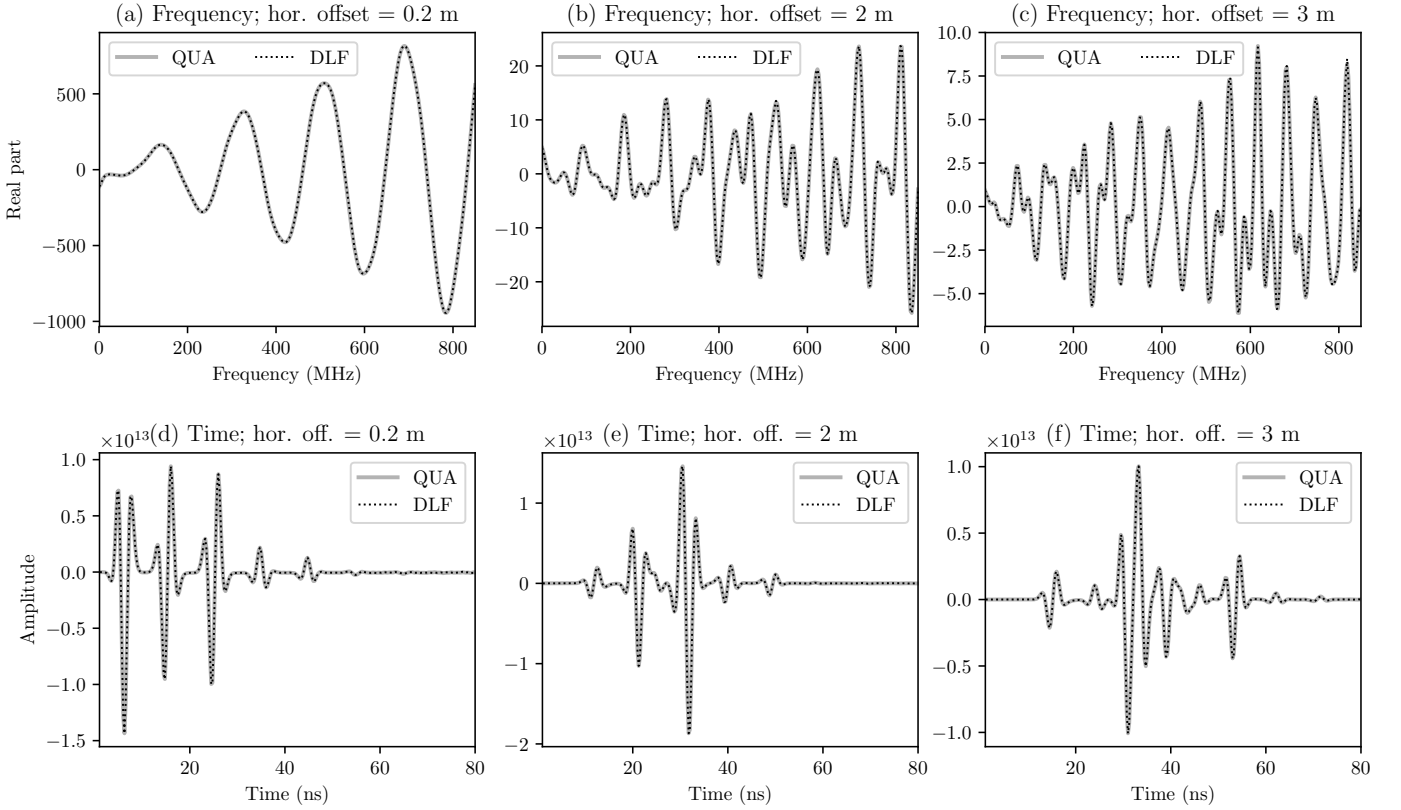


Figure 7: The real-part frequency-domain and the time-domain responses for offsets of (a/d) 0.2 m, (b/e) 2.0 m, and (c/f) 3.0 m.

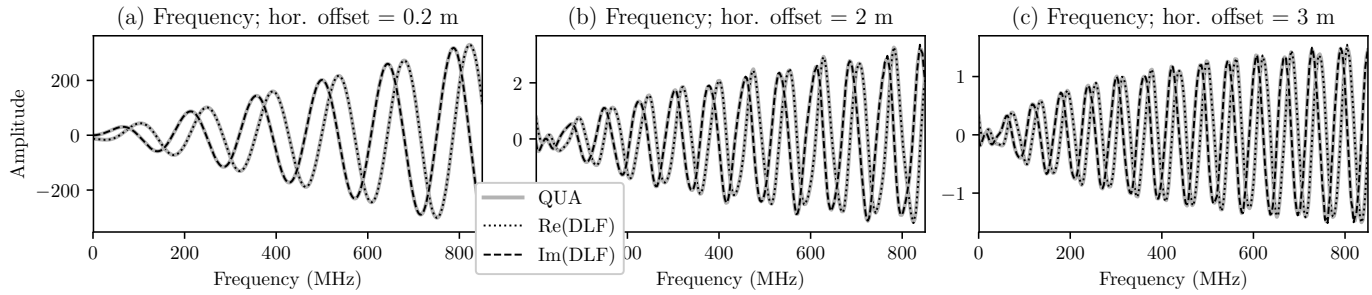


Figure 8: The real and imaginary parts of the frequency-domain response for the model given in Figure 6 (a) with swapped first and second layers for offsets of (a) 0.2 m, (b) 2.0 m, and (c) 3.0 m.

form) using either analytical transform pairs or 1D sub-surface models together with the EM-modeler `empymod`. The code is available from GitHub in the add-on repository of `empymod`, called `empyscripts`, from version 0.1.2 onwards.

The presented 201 pt filter achieves more precise results in the three presented CSEM cases than other filters, and is included in `empymod` from version 1.4.5 onwards. However, as with any digital filter, the quality depends heavily on the model, and this new filter might or might not behave that well for other models.

The shown GPR result shows that the digital linear filter method can also be used for wave phenomena, not only for the diffusive approximation limit of low frequency EM modeling.

We expect the presented algorithm is useful for at least 3 scenarios:

1. Provide a fast method to design problem-specific filters. For bigger inversion projects (such as, for instance, massive stochastic CSEM inversions) a purpose designed, short filter might save much more time than it costs to design it. This could even be integrated into inversion codes, as an optional pre-inversion step.
2. Extend the filter method to new areas, namely higher frequencies and acoustic and elastic wavefields.
3. Raise a new interest for digital linear filters in geophysics, by making it very easy for anyone to play around, create their own filters, and get a better understanding of it. We are sure there are many great filters to be discovered.

REFERENCES

- Anderson, W. L., 1973, Fortran IV programs for the determination of the transient tangential electric field and vertical magnetic field about a vertical magnetic dipole for an m -layer stratified earth by numerical integration and digital linear filtering: USGS, **PB221240**.
- , 1975, Improved digital filters for evaluating Fourier and Hankel transform integrals: USGS, **PB242800**. (<https://pubs.er.usgs.gov/publication/70045426>).
- , 1979, Numerical integration of related Hankel transforms of orders 0 and 1 by adaptive digital filtering: *Geophysics*, **44**, 1287–1305. (doi: [10.1190/1.1441007](https://doi.org/10.1190/1.1441007)).
- , 1982, Fast Hankel transforms using related and lagged convolutions: *ACM Trans. Math. Softw.*, **8**, 344–368. (doi: [10.1145/356012.356014](https://doi.org/10.1145/356012.356014)).
- , 1984, On: “Numerical integration of related Hankel transforms by quadrature and continued fraction expansion” by Chave (1983): *Geophysics*, **49**, 1811–1812. (doi: [10.1190/1.1441595](https://doi.org/10.1190/1.1441595)).
- , 1989, A hybrid fast Hankel transform algorithm for electromagnetic modeling: *Geophysics*, **54**, 263–266. (doi: [10.1190/1.1442650](https://doi.org/10.1190/1.1442650)).
- Bernabini, M., and E. Cardarelli, 1978, The use of filtered Bessel functions in direct interpretation of geoelectrical soundings: *Geophysical Prospecting*, **26**, 841–852. (doi: [10.1111/j.1365-2478.1978.tb01636.x](https://doi.org/10.1111/j.1365-2478.1978.tb01636.x)).
- Bichara, M., and J. Lakshmanan, 1976, Fast automatic processing of resistivity soundings*: *Geophysical Prospecting*, **24**, 354–370. (doi: [10.1111/j.1365-2478.1976.tb00932.x](https://doi.org/10.1111/j.1365-2478.1976.tb00932.x)).
- Chave, A. D., 1983, Numerical integration of related Hankel transforms by quadrature and continued fraction expansion: *Geophysics*, **48**, 1671–1686. (doi: [10.1190/1.1441448](https://doi.org/10.1190/1.1441448)).
- Christensen, N. B., 1990, Optimized fast Hankel transform filters: *Geophysical Prospecting*, **38**, 545–568. (doi: [10.1111/j.1365-2478.1990.tb01861.x](https://doi.org/10.1111/j.1365-2478.1990.tb01861.x)).
- Das, U. C., 1982, Designing digital linear filters for computing resistivity and electromagnetic sounding curves: *Geophysics*, **47**, 1456–1459. (doi: [10.1190/1.1441295](https://doi.org/10.1190/1.1441295)).
- , 1984, A single digital linear filter for computations in electrical methods—a unifying approach: *Geophysics*, **49**, 1115–1118. (doi: [10.1190/1.1441726](https://doi.org/10.1190/1.1441726)).
- Das, U. C., and D. P. Ghosh, 1974, The determination of filter coefficients for the computation of standard curves for dipole resistivity sounding over layered earth by linear digital filtering: *Geophysical Prospecting*, **22**, 765–780. (doi: [10.1111/j.1365-2478.1974.tb00117.x](https://doi.org/10.1111/j.1365-2478.1974.tb00117.x)).
- Das, U. C., D. P. Ghosh, and D. T. Biewinga, 1974, Trans-

- formation of dipole resistivity sounding measurements over layered earth by linear digital filtering: *Geophysical Prospecting*, **22**, 476–489. (doi: [10.1111/j.1365-2478.1974.tb00100.x](https://doi.org/10.1111/j.1365-2478.1974.tb00100.x)).
- Das, U. C., and S. K. Verma, 1980, Digital linear filter for computing type curves for the two-electrode system of resistivity sounding: *Geophysical Prospecting*, **28**, 610–619. (doi: [10.1111/j.1365-2478.1980.tb01246.x](https://doi.org/10.1111/j.1365-2478.1980.tb01246.x)).
- , 1981a, Numerical considerations on computing the EM response of three-dimensional inhomogeneities in a layered earth: *Geophysical Journal International*, **66**, 733–740. (doi: [10.1111/j.1365-246X.1981.tb04897.x](https://doi.org/10.1111/j.1365-246X.1981.tb04897.x)).
- , 1981b, The versatility of digital linear filters used in computing resistivity and em sounding curves: *Geoexploration*, **18**, 297–310. (doi: [10.1016/0016-7142\(81\)90059-4](https://doi.org/10.1016/0016-7142(81)90059-4)).
- , 1982, Electromagnetic response of an arbitrarily shaped three-dimensional conductor in a layered earth — numerical results: *Geophysical Journal International*, **69**, 55–66. (doi: [10.1111/j.1365-246X.1982.tb04935.x](https://doi.org/10.1111/j.1365-246X.1982.tb04935.x)).
- Davis, P. A., S. A. Greenhalgh, and N. P. Merrick, 1980, Resistivity sounding computations with any array using a single digital filter: *Exploration Geophysics*, **11**, 54–62. (doi: [10.1071/EG980054](https://doi.org/10.1071/EG980054)).
- Ghosh, D. P., 1970, The application of linear filter theory to the direct interpretation of geoelectrical resistivity measurements: Ph.D. Thesis, TU Delft. (uuid: [88a568bb-ebee-4d7b-92df-6639b42da2b2](https://nbn-resolving.org/urn:nbn:nl:ui:88a568bb-ebee-4d7b-92df-6639b42da2b2)).
- , 1971a, The application of linear filter theory to the direct interpretation of geoelectrical resistivity sounding measurements: *Geophysical Prospecting*, **19**, 192–217. (doi: [10.1111/j.1365-2478.1971.tb00593.x](https://doi.org/10.1111/j.1365-2478.1971.tb00593.x)).
- , 1971b, Inverse filter coefficients for the computation of apparent resistivity standard curves for a horizontally stratified earth: *Geophysical Prospecting*, **19**, 769–775. (doi: [10.1111/j.1365-2478.1971.tb00915.x](https://doi.org/10.1111/j.1365-2478.1971.tb00915.x)).
- Guptasarma, D., 1982, Optimization of short digital linear filters for increased accuracy: *Geophysical Prospecting*, **30**, 501–514. (doi: [10.1111/j.1365-2478.1982.tb01320.x](https://doi.org/10.1111/j.1365-2478.1982.tb01320.x)).
- Guptasarma, D., and B. Singh, 1997, New digital linear filters for Hankel J0 and J1 transforms: *Geophysical Prospecting*, **45**, 745–762. (doi: [10.1046/10.1046/j.1365-2478.1997.500292.x](https://doi.org/10.1046/10.1046/j.1365-2478.1997.500292.x)).
- Hunziker, J., J. Thorbecke, and E. Slob, 2015, The electromagnetic response in a layered vertical transverse isotropic medium: A new look at an old problem: *Geophysics*, **80**, no. 1, F1–F18. (doi: [10.1190/geo2013-0411.1](https://doi.org/10.1190/geo2013-0411.1)).
- Johansen, H. K., 1975, An interactive computer/graphic-display-terminal system for interpretation of resistivity soundings: *Geophysical Prospecting*, **23**, 449–458. (doi: [10.1111/j.1365-2478.1975.tb01541.x](https://doi.org/10.1111/j.1365-2478.1975.tb01541.x)).
- Johansen, H. K., and K. Sørensen, 1979, Fast Hankel transforms: *Geophysical Prospecting*, **27**, 876–901. (doi: [10.1111/j.1365-2478.1979.tb01005.x](https://doi.org/10.1111/j.1365-2478.1979.tb01005.x)).
- Key, K., 2009, 1D inversion of multicomponent, multifrequency marine CSEM data: Methodology and synthetic studies for resolving thin resistive layers: *Geophysics*, **74**, no. 2, F9–F20. (doi: [10.1190/1.3058434](https://doi.org/10.1190/1.3058434)).
- , 2012, Is the fast Hankel transform faster than quadrature?: *Geophysics*, **77**, no. 3, F21–F30. (doi: [10.1190/GEO2011-0237.1](https://doi.org/10.1190/GEO2011-0237.1)).
- Koefoed, O., 1968, The application of the kernel function in interpreting geoelectrical resistivity measurements: Gebrüder Borntraeger. (ISBN: 9783443130022).
- , 1970, A fast method for determining the layer distribution from the raised kernel function in geoelectrical sounding: *Geophysical Prospecting*, **18**, 564–570. (doi: [10.1111/j.1365-2478.1970.tb02129.x](https://doi.org/10.1111/j.1365-2478.1970.tb02129.x)).
- , 1972, A note on the linear filter method of interpreting resistivity sounding data: *Geophysical Prospecting*, **20**, 403–405. (doi: [10.1111/j.1365-2478.1972.tb00643.x](https://doi.org/10.1111/j.1365-2478.1972.tb00643.x)).
- , 1976, Error propagation and uncertainty in the interpretation of resistivity sounding data: *Geophysical Prospecting*, **24**, 31–48. (doi: [10.1111/j.1365-2478.1976.tb00383.x](https://doi.org/10.1111/j.1365-2478.1976.tb00383.x)).
- Koefoed, O., and F. J. H. Dirks, 1979, Determination of resistivity sounding filters by the Wiener-Hopf least-squares method: *Geophysical Prospecting*, **27**, 245–250. (doi: [10.1111/j.1365-2478.1979.tb00968.x](https://doi.org/10.1111/j.1365-2478.1979.tb00968.x)).
- Koefoed, O., D. P. Ghosh, and G. J. Polman, 1972, Computation of type curves for electromagnetic depth sounding with a horizontal transmitting coil by means of a digital linear filter: *Geophysical Prospecting*, **20**, 406–420. (doi: [10.1111/j.1365-2478.1972.tb00644.x](https://doi.org/10.1111/j.1365-2478.1972.tb00644.x)).
- Kong, F. N., 2007, Hankel transform filters for dipole antenna radiation in a conductive medium: *Geophysical Prospecting*, **55**, 83–89. (doi: [10.1111/j.1365-2478.2006.00585.x](https://doi.org/10.1111/j.1365-2478.2006.00585.x)).
- Kruglyakov, M., and L. Bloshanskaya, 2017, High-performance parallel solver for integral equations of electromagnetics based on Galerkin method: *Mathematical Geosciences*, **49**, 751–776. (doi: [10.1007/s11004-017-9677-y](https://doi.org/10.1007/s11004-017-9677-y)).
- Kumar, R., and U. C. Das, 1977, Transformation of dipole to Schlumberger sounding curves by means of digital linear filters: *Geophysical Prospecting*, **25**, 780–789. (doi: [10.1111/j.1365-2478.1977.tb01204.x](https://doi.org/10.1111/j.1365-2478.1977.tb01204.x)).
- , 1978, Transformation of Schlumberger apparent resistivity to dipole apparent resistivity over layered earth by the application of digital linear filters: *Geophysical Prospecting*, **26**, 352–358. (doi: [10.1111/j.1365-2478.1978.tb01598.x](https://doi.org/10.1111/j.1365-2478.1978.tb01598.x)).
- Mohsen, A. A., and E. A. Hashish, 1994, The fast Hankel transform: *Geophysical Prospecting*, **42**, 131–139. (doi: [10.1111/j.1365-2478.1994.tb00202.x](https://doi.org/10.1111/j.1365-2478.1994.tb00202.x)).
- Murakami, Y., and T. Uchida, 1982, Accuracy of the linear filter coefficients determined by the iteration of the least-squares method: *Geophysics*, **47**, 244–256. (doi: [10.1190/1.1441331](https://doi.org/10.1190/1.1441331)).
- Newman, G. A., G. W. Hohmann, and W. L. Anderson, 1986, Transient electromagnetic response of a three-

- dimensional body in a layered earth: *Geophysics*, **51**, 1608–1627. (doi: [10.1190/1.1442212](https://doi.org/10.1190/1.1442212)).
- Nissen, J., and T. Enmark, 1986, An optimized digital filter for the Fourier transform: *Geophysical Prospecting*, **34**, 897–903. (doi: [10.1111/j.1365-2478.1986.tb00500.x](https://doi.org/10.1111/j.1365-2478.1986.tb00500.x)).
- Niwas, S., 1975, Direct interpretation of geoelectric measurements by the use of linear filter theory: *Geophysics*, **40**, 121–122. (doi: [10.1190/1.1440510](https://doi.org/10.1190/1.1440510)).
- Nyman, D. C., and M. Landisman, 1977, VES dipole-dipole filter coefficients: *Geophysics*, **42**, 1037–1044. (doi: [10.1190/1.1440763](https://doi.org/10.1190/1.1440763)).
- O'Neill, D., 1975, Improved linear filter coefficients for application in apparent resistivity computations: *Exploration Geophysics*, **6**, 104–109. (doi: [10.1071/EG975104](https://doi.org/10.1071/EG975104)).
- O'Neill, D. J., and N. P. Merrick, 1984, A digital linear filter for resistivity sounding with a generalized electrode array: *Geophysical Prospecting*, **32**, 105–123. (doi: [10.1111/j.1365-2478.1984.tb00720.x](https://doi.org/10.1111/j.1365-2478.1984.tb00720.x)).
- Pekeris, C. L., 1940, Direct method of interpretation in resistivity prospecting: *Geophysics*, **5**, 31–42. (doi: [10.1190/1.1441791](https://doi.org/10.1190/1.1441791)).
- Raiche, A., F. Sugeng, and G. Wilson, 2007, Practical 3D EM inversion - the P223F software suite: *ASEG Technical Program Expanded Abstracts*, 1–4. (doi: [10.1071/ASEG2007ab114](https://doi.org/10.1071/ASEG2007ab114)).
- Slichter, L. B., 1933, The interpretation of the resistivity prospecting method for horizontal structures: *Physics*, **4**, 307–322. (doi : [10.1063/1.1745198](https://doi.org/10.1063/1.1745198)).
- Sørensen, K. I., and N. B. Christensen, 1994, The fields from a finite electrical dipole—a new computational approach: *Geophysics*, **59**, 864–880. ([10.1190/1.1443646](https://doi.org/10.1190/1.1443646)).
- Verma, R. K., and O. Koefoed, 1973, A note on the linear filter method of computing electromagnetic sounding curves: *Geophysical Prospecting*, **21**, 70–76. (doi: [10.1111/j.1365-2478.1973.tb00015.x](https://doi.org/10.1111/j.1365-2478.1973.tb00015.x)).
- Werthmüller, D., 2017, An open-source full 3D electromagnetic modeler for 1D VTI media in Python: *empymod*: *Geophysics*, **82**, no. 6, WB9–WB19. (doi: [10.1190/geo2016-0626.1](https://doi.org/10.1190/geo2016-0626.1)).